CrossMark

The Great Dimming of Betelgeuse from the VLT/VLTI

**M. Montargès[1], E. Cannon[2], E. Lagadec[3], A. de Koter[4,2],
P. Kervella[1], J. Sanchez-Bermudez[5,6], C. Paladini[7],
F. Cantalloube[8], L. Decin[2,9], P. Scicluna[7], K. Kravchenko[10],
A. K. Dupree[11] S. Ridgway[12], M. Wittkowski[13], N. Anugu[14,15],
R. Norris[16], G. Rau[17,18], G. Perrin[1], A. Chiavassa[3], S. Kraus[15],
J. D. Monnier[19], F. Millour[3], J.-B. Le Bouquin[19,20], X. Haubois[7],
B. Lopez[3], P. Stee[3] and W. Danchi[17].**

[1]LESIA, Observatoire de Paris, Université PSL, CNRS, Sorbonne Université, Université de Paris, 5 place Jules Janssen, 92195 Meudon, France
email: miguel.montarges@observatoiredeparis.psl.eu

[2]Institute of Astronomy, KU Leuven, Celestijnenlaan 200D B2401, 3001 Leuven, Belgium

[3]Université Côte d'Azur, Observatoire de la Côte d'Azur, CNRS, Laboratoire Lagrange, Bd de l'Observatoire, CS 34229, 06304 Nice cedex 4, France

[4]Anton Pannenkoek Institute for Astronomy, University of Amsterdam, 1090 GE, Amsterdam, The Netherlands

[5]Max Planck Institute for Astronomy, Königstuhl 17, 69117, Heidelberg, Germany

[6]Instituto de Astronomía, Universidad Nacional Autónoma de México, Apdo. Postal 70264, Ciudad de México, 04510, México

[7]European Southern Observatory, Alonso de Cordova 3107, Vitacura, Santiago, Chile

[8]Aix Marseille Université, CNRS, LAM (Laboratoire d'Astrophysique de Marseille) UMR 7326, 13388, Marseille, France

[9]School of Chemistry, University of Leeds, Leeds LS2 9JT, UK

[10]Max Planck Institute for extraterrestrial Physics, Giessenbachstraße 1, D-85748 Garching, Germany

[11]Center for Astrophysics, Harvard & Smithsonian, 60 Garden Street, Cambridge, MA 02138, USA

[12]NSF's National Optical-Infrared Astronomy Research Laboratory, PO Box 26732, Tucson, AZ 85726-6732, USA

[13]European Southern Observatory, Karl-Schwarzschild-Str. 2, 85748, Garching bei München, Germany

[14]Steward Observatory, 933 N. Cherry Avenue, University of Arizona, Tucson, AZ, 85721, USA

[15]University of Exeter, School of Physics and Astronomy, Stocker Road, Exeter, EX4 4QL, UK

[16]Physics Department, New Mexico Institute of Mining and Technology, 801 Leroy Place, Socorro, NM 87801, USA

[17]NASA Goddard Space Flight Center, Exoplanets & Stellar Astrophysics Laboratory, Code 667, Greenbelt, MD 20771, USA

[18]Department of Physics, Catholic University of America, Washington, DC 20064, USA

[19]Department of Astronomy, University of Michigan, Ann Arbor, MI, 48109, USA

[20]Univ. Grenoble Alpes, CNRS, IPAG, 38000 Grenoble, France

Abstract. From November 2019 to April 2020, the prototypical red supergiant Betelgeuse experienced an unexpected and historic dimming. This event was observed worldwide by astrophysicists, and also by the general public with the naked eye. We present here the results of our observing campaign with ESO's VLT and VLTI in the visible and infrared domains. The observations with VLT/SPHERE-ZIMPOL, VLT/SPHERE-IRDIS, VLTI/GRAVITY and VLTI/MATISSE provide spatially resolved diagnostics of this event. Using PHOENIX atmosphere models and RADMC3D dust radiative transfer simulations, we built a consistent model reproducing the images and the photometry.

Keywords. Stars, Stellar evolution, Time-domain astronomy, Transient astrophysical phenomena, Stars: individual: Betelgeuse, supergiants, Stars: mass-loss, Stars: imaging, Techniques: high angular resolution.

1. Introduction

Mass loss of red supergiants (RSG) is far from being understood. In particular, the triggering mechanism that allows the material to escape the photosphere remains unknown. Two main scenarios have been proposed to explain the origin of the outflow: (1) the combined action of a lowering of the effective gravity through turbulent velocities initiated by giant convective cells (Kee et al. 2021), possibly supported by radiative pressure on molecular lines (Josselin & Plez 2007), and (2) Alfvén waves dissipation through the chromosphere (Airapetian et al. 2000). Polarimetric adaptive-optics imaging in the visible revealed dust clumps at a few stellar radii from the photosphere (Kervella et al. 2016 and Cannon et al. 2021), pointing to an episodic and non-homogeneous mass loss, further complicating the picture.

High angular resolution observations represent the best tool to find the missing mechanism by observing material ejection close to the photosphere. Being the second closest RSG (222^{+48}_{-34} pc; see Harper et al. 2017 and Joyce et al. 2020), Betelgeuse (α Ori) is among the preferred targets for such observations, and often considered to be the prototypical star of this luminosity class. Its visual light curve shows two main periods of $\sim 400-420$, and ~ 2100 days respectively (Stothers 2010). At the end of 2019, while it was on its way to its anticipated minimum, its brightness decreased faster than usual (Guinan et al. 2019). We now know that this was the beginning of what has been called 'the Great Dimming of Betelgeuse' with the star reaching its historic visible minimum on 7-13 February 2020 (Guinan et al. 2020 and Fig. 1), few days after the expected minimum. Its V band magnitude was then $V = 1.614 \pm 0.008$ mag.

Here we provide a concise summary of the main findings of the refereed article Montargès et al. (2021), that have been presented during the conference.

2. Observations

We obtained observations of Betelgeuse one year before the 'Great Dimming'. By chance these have been scheduled exactly at the previous light minimum. The VLT/SPHERE (Beuzit et al. 2019) data were obtained on the night of January 1st 2019, both with the Zurich Imaging Polarimeter (ZIMPOL, Schmid et al. 2018) in visible polarimetric imaging, and with the infra-red dual imaging and spectrograph (IRDIS, Dohlen et al. 2008) for infrared sparse aperture masking (SAM, Cheetham et al. 2016). VLTI/GRAVITY (Gravity Collaboration et al. 2017) data were secured in the compact configuration of the auxiliary telescopes (A0-B2-D0-C1) on 20th January 2019. Following successful Director Discretionary Time proposals, observations were executed during the 'Great Dimming' on 14th February 2020 with VLTI/GRAVITY, 27th December 2019
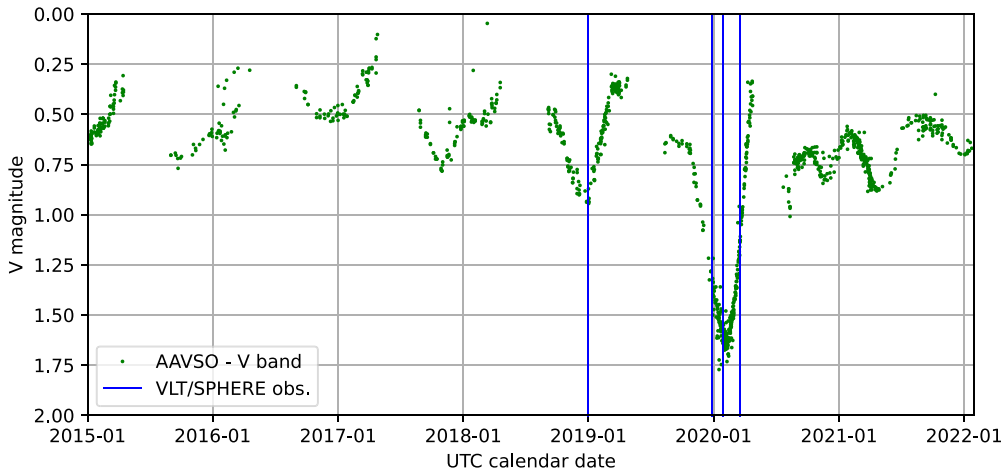
Figure 1. V band light curve of Betelgeuse between 2015 and 2022 from the American Association of Variable Star Observers (AAVSO) measurements. The vertical lines correspond to the dates of the VLT/SPHERE-ZIMPOL images.

with VLT/SPHERE-IRDIS, and 27$^{\text{th}}$ December 2019 (before the light minimum), 28$^{\text{th}}$ January 2020 (at the light minimum), and 18$^{\text{th}}$, 19$^{\text{th}}$ and 21$^{\text{st}}$ March 2020 (after the light minimum) with VLT/SPHERE-ZIMPOL.

The GRAVITY data, combined with the short baseline IRDIS SAM observations, allow to precisely measure the angular diameter in the near infrared (NIR). The visible ZIMPOL direct imaging spatially resolves the photosphere of the star, owing to its large angular diameter (Sect. 59).

The data reduction and calibration are described in details in Montargès et al. (2021).

3. Measuring the angular diameter with optical interferometry

The 'Great Dimming' could have been caused by a change of size of Betelgeuse. The angular diameter is also an important input of any numerical model. We used the combination of interferometric observables from VLT/SPHERE-IRDIS (Cnt_K2 filter) in SAM mode and VLTI/GRAVITY (in the K band continuum at $2.22 - 2.28$ μm) to measure it. The angular diameters values obtained are $\theta_{\text{UD}} = 42.61 \pm 0.05$ mas (reduced $\chi^2 = 26.5$) before the Dimming, and $\theta_{\text{UD}} = 42.11 \pm 0.05$ mas (reduced $\chi^2 = 46.3$) during the Dimming. An attempt to fit the data with a power-law limb-darkened disk does not change significantly the reduced χ^2 values, nor the angular diameter.

The angular diameter variation is far from the 30% decrease that would be necessary to fully reproduce the 'Great Dimming'. It is consistent with the variations registered over the previous decades (Ohnaka et al. 2009).

4. Spatially resolved imaging of the photosphere

The spatially resolved images of Betelgeuse in the visible (Fig. 2) reveal an almost spherical photosphere before (January 2019) the 'Great Dimming', slightly elongated in the North-East to South-West direction. During the 'Great Dimming', the Southern hemisphere appears much dimmer than the rest of the star. This is modeled in the following sections.
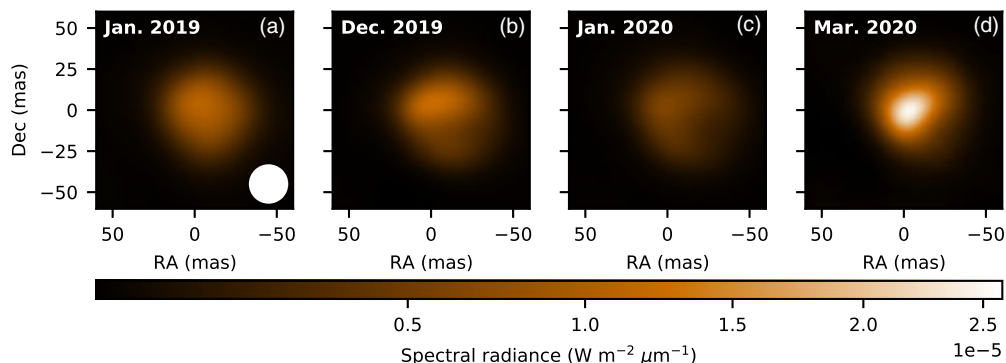
Figure 2. Deconvolved VLT/SPHERE-ZIMPOL observations of Betelgeuse in the Cnt_Hα filter (644.9 nm). North is up; east is left. The beam size of ZIMPOL is indicated by the white disk in panel a. A power-law scale intensity with an index of 0.65 is used to enhance the contrast. Panel a: January 2019. b: December 2019. c: January 2020. d: March 2020.

Table 1. Best matching parameters of the synthetic cool patch PHOENIX models with the ZIMPOL observations. $\log \mathcal{L}$ is the log-likelihood. See Sect. 33 for the definition of the parameters.

Parameter	December 2019	January 2020	March 2020
x_p (mas)	-7.1	-2.4	-28.4
y_p (mas)	-14.2	-2.4	-35.6
r_p (mas)	23.7	19.0	45.0
T_{hot} (K)	$3,700$	$3,700$	$3,700$
T_{cool} (K)	$3,400$	$3,400$	$3,200$
$\log \mathcal{L}$	-8.8×10^6	-5.5×10^7	-4.0×10^7

4.1. *A constant dust component in the line of sight*

It has been known for many decades that Betelgeuse is permanently surrounded by a relatively thin dusty envelope (see for example Verhoelst et al. 2009 and Kervella et al. 2011 and references therein). In order to determine the dust contribution to the 'Great Dimming' (if any), it is important to determine the dust component already detectable in the January 2019 images.

In order to estimate the contribution of the dust in the pre-dimming images, we derived the photometry from the SPHERE-ZIMPOL images, and collected the contemporaneous data from the American Association of Variable Stars Observers (AAVSO). We modeled these photometric measurements using a Cardelli extinction law (Cardelli et al. 1989) applied to a PHOENIX atmosphere of a RSG (Lançon et al. 2007) at 3600 K. We derive $R_V = 4.2$ and $A_V = 0.65$. Hereafter we consider that the 'Great Dimming' event happens in addition to this pre-existing extinction.

4.2. *Photospheric cool spot model*

We first attempt to reproduce the 'Great Dimming' by considering a cool patch on the photosphere of Betelgeuse. We model this by creating a composite stellar disk from PHOENIX atmosphere models (Lançon et al. 2007) at different temperatures.

Three parameters fully define the cool patch in addition to its temperature: its center position on the stellar disk (x_p, y_p), and its size r_p. The modeling details are available in Montargès et al. (2021). Table 1 shows the best match parameters, and the corresponding images are shown in Fig. 3. The photometry is plotted on Fig. 4.
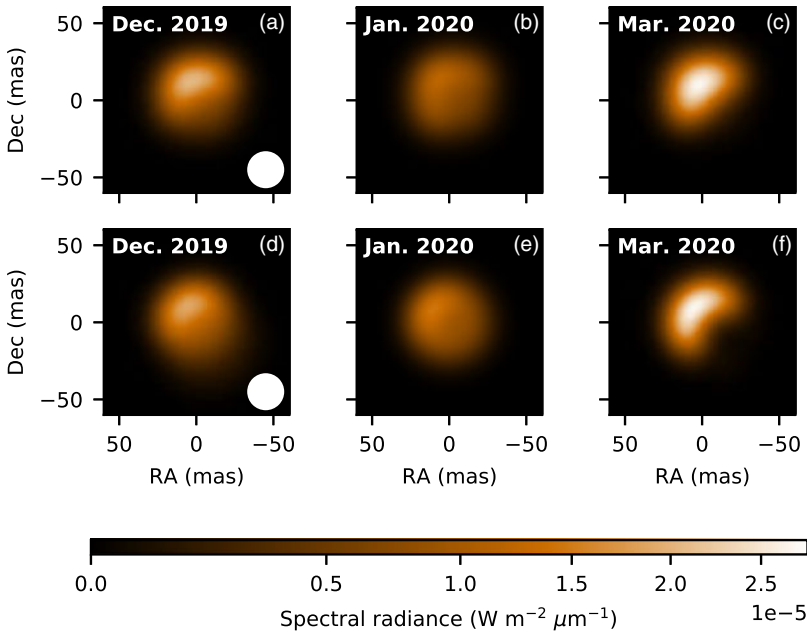
Figure 3. Best matching models for the ZIMPOL images in the Cnt_Hα filter (644.9 nm). The upper images correspond to the cool spot PHOENIX model, the lower images to the dusty clump RADMC3D simulations.

Here we have only assessed the compatibility of a cool spot model with the 'Great Dimming'. Precisely constraining the temperatures of the photosphere and the spot would require multi-spectral spatially resolved imaging,

4.3. *Dusty clump model*

Another scenario to explain the 'Great Dimming' of Betelgeuse could be the formation of a cloud of dust in the line of sight. We explore this hypothesis through RADMC3D (Dullemond 2012) radiative transfer simulations.

In our models we consider the x axis to be oriented West to East, the y axis South to North, and the z axis towards the observer. The spherical dust clump is centred at (x_c, y_c, z_c), r_c being its radius, and possess a constant dust density of ρ_0. We consider the dust to be made of $MgFeSiO_4$ (Jaeger et al. 1994; Dorschner et al. 1995). We set the grain size to have maximum absorption by the dust clump in the visible, which is achieved adopting grain radii in the range 0.18 to 0.24 μm, following a gaussian size distribution.

We produced a grid of simulations to be matched with the SPHERE-ZIMPOL images and their photometry. The procedure did not converge for the images taken in January and March 2020. For these two epochs, we used best guesses obtained by manually matching the observables. The results are summarized in Table 2, and the images are shown in Fig. 3. The corresponding photometry is represented on Fig. 4.

5. Conclusion

Both types of models (cool patch and dusty clump) are able to reproduce the images of the 'Great Dimming' obtained by VLT/SPHERE-ZIMPOL. However, both are not fully reproducing the SED, particularly in the NIR (Fig. 4). Comparison with the other observations of the 'Great Dimming' are discussed in Montargès et al. (2021). In order

Table 2. Best matching parameters for the RADMC3D clump simulations with the ZIMPOL observations. See Sect. 34 for the definition of the parameters.

Parameter	December 2019	January 2020	March 2020
x_c (au)	-1.9	-0.8	-1.9
y_c (au)	-3.0	-0.6	-1.8
z_c (au)	12.5	20.0	20.0
r_c (au)	6.5	5.0	4.5
ρ_0 (g cm^{-3})	3.2×10^{-19}	4.0×10^{-19}	2.0×10^{-18}
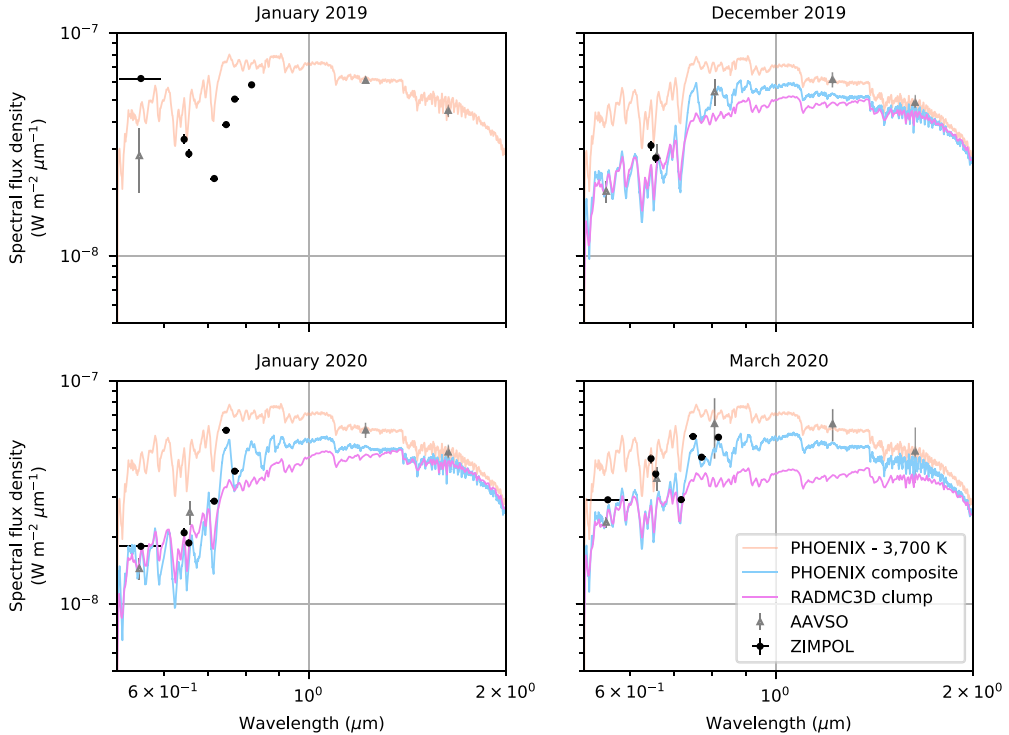
Figure 4. Observed photometry and modeled SEDs for Betelgeuse before (a), and during the 'Great Dimming' (b, c, and d). The black dots correspond to the ZIMPOL photometry, the gray triangles to the AAVSO measurements. The orange curve represents the SED of a PHOENIX 15 M$_\odot$ RSG with T$_{eff}$ = 3700 K. The blue curve corresponds to the best matching PHOENIX cool patch model, and the purple curve to the best dusty clump RADMC3D simulation.

to attempt a full explanation of the event, and to frame it within the general pulsation pattern of Betelgeuse (the exceptional light minimum happend 4 days later than the expected 2020 minimum), we conclude that both scenarios happened consecutively. A gas cloud had been expelled by the star months or years before the event. In late 2019 a cool patch appeared on the visible hemisphere of Betelgeuse, which triggered dust nucleation in the dust cloud located above the photosphere. The 'Great Dimming' is the combination of the cool spot and the dusty clump, which explains why each hypothesis cannot fully explain the observations individually.

References

Airapetian, V. S., Ofman, L., Robinson, R. D., Carpenter, K., & Davila, J. 2000, *ApJ* 528, 965
Beuzit, J. L., Vigan, A., Mouillet, D., et al. 2019, *A&A* 631, A155
Cannon, E., Montargès, M., de Koter, A., et al. 2021, *MNRAS* 502(1), 369
Cardelli, J. A., Clayton, G. C., & Mathis, J. S. 1989, *ApJ* 345, 245

Cheetham, A. C., Girard, J., Lacour, S., et al. 2016, in F. Malbet, M. J. Creech-Eakman, & P. G. Tuthill (eds.), *Optical and Infrared Interferometry and Imaging V*, Vol. 9907 of *Society of Photo-Optical Instrumentation Engineers (SPIE) Conference Series*, p. 99072T

Dohlen, K., Langlois, M., Saisse, M., et al. 2008, in I. S. McLean & M. M. Casali (eds.), *Ground-based and Airborne Instrumentation for Astronomy II*, Vol. 7014 of *Society of Photo-Optical Instrumentation Engineers (SPIE) Conference Series*, p. 70143L

Dorschner, J., Begemann, B., Henning, T., Jaeger, C., & Mutschke, H. 1995, *A&A* 300, 503

Dullemond, C. P. 2012, *RADMC-3D: A multi-purpose radiative transfer tool*, Astrophysics Source Code Library

Gravity Collaboration, Abuter, R., Accardo, M., et al. 2017, *A&A* 602, A94

Guinan, E., Wasatonic, R., Calderwood, T., & Carona, D. 2020, *The Astronomer's Telegram* 13512, 1

Guinan, E. F., Wasatonic, R. J., & Calderwood, T. J. 2019, *The Astronomer's Telegram* 13341, 1

Harper, G. M., Brown, A., Guinan, E. F., et al. 2017, *AJ* 154, 11

Jaeger, C., Mutschke, H., Begemann, B., Dorschner, J., & Henning, T. 1994, *A&A* 292, 641

Josselin, E. & Plez, B. 2007, *A&A* 469, 671

Joyce, M., Leung, S.-C., Molnár, L., et al. 2020, *ApJ* 902(1), 63

Kee, N. D., Sundqvist, J. O., Decin, L., de Koter, A., & Sana, H. 2021, *A&A* 646, A180

Kervella, P., Lagadec, E., Montargès, M., et al. 2016, *A&A* 585, A28

Kervella, P., Perrin, G., Chiavassa, A., et al. 2011, *A&A* 531, A117

Lançon, A., Hauschildt, P. H., Ladjal, D., & Mouhcine, M. 2007, *A&A* 468, 205

Montargès, M., Cannon, E., Lagadec, E., et al. 2021, *Nature* 594(7863), 365

Ohnaka, K., Hofmann, K.-H., Benisty, M., et al. 2009, *A&A* 503, 183

Schmid, H. M., Bazzon, A., Roelfsema, R., et al. 2018, *A&A* 619, A9

Stothers, R. B. 2010, *ApJ* 725, 1170

Verhoelst, T., van der Zypen, N., Hony, S., et al. 2009, *A&A* 498, 127